Quantitative Analysis of a RNA-Cleaving DNA Catalyst Obtained via in Vitro Selection†

Matthew A. Carrigan,*,‡,§ Alonso Ricardo,§ Darwin N. Ang,§ and Steven A. Benner*,‡,§

Foundation for Applied Molecular Evolution, Incorporated, Post Office Box 13174, Gainesville, Florida 32604, and Department of Chemistry, 432 Leigh Hall, University of Florida, Gainesville, Florida 32611

Received January 13, 2004; Revised Manuscript Received July 7, 2004

ABSTRACT: In vitro selections performed in the presence of Mg^{2+} generated DNA sequences capable of cleaving an internal ribonucleoside linkage. Several of these, surprisingly, displayed intermolecular catalysis and catalysis independent of Mg^{2+}, features that the selection protocol was not explicitly designed to select. A detailed physical organic analysis was applied to one of these DNAzymes, termed **614**. First, the progress curve for the reaction was dissected to identify factors that prevented the molecule from displaying clean first-order transformation kinetics and 100% conversion. Several factors were identified and quantitated, including (a) competitive intra- and intermolecular rate processes, (b) alternative reactive and unreactive conformations, and (c) mutations within the catalyst. Other factors were excluded, including "approach to equilibrium" kinetics and product inhibition. The possibility of complementary strand inhibition was demonstrated but was shown to not be a factor under the conditions of these experiments. The rates of the intra- and intermolecular processes were compared, and saturation models for the intermolecular process were built. The rate-limiting step for the intermolecular reaction was found to be the association/folding of the enzyme with the substrate and not the cleavage step. The DNAzyme **614** is more active in trans than in cis and more active at temperatures below the selection temperature than at the selection temperature. Many of these properties have not been reported in similar systems; these results therefore expand the phenomenology known for this class of DNA-based catalysts. A brief survey of other catalysts arising from this selection found other Mg^{2+}-independent DNAzymes and provided a preliminary view of the ruggedness of the landscape, relating function to structure in sequence space. Hypotheses are suggested to account for the fact that a selection in the presence of Mg^{2+} did not exploit this Mg^{2+}. This study of a specific catalytically active DNAzyme is an example of studies that will be necessary generally to permit in vitro selection to help us understand the distribution of function in sequence space.

Szostak, Joyce, Ellington, and others, 10 years ago, applied in vitro selection to libraries of nucleic acids to extract nucleic acids that catalyze simple reactions, such as RNA ligation (*1*) and RNA cleavage (*2*). This work opened the possibility of using in vitro selection to ask quantitative questions about the performance of these catalysts. This includes questions concerning the mechanism of specific nucleic acid enzymes, as well as broader questions, such as how functional behavior is distributed in nucleic acid sequence "space" and whether adding chemical functionality to nucleic acids, either by modifying the nucleobases or by adding cofactors, can enhance the catalytic potential of a nucleic acid library (*3*−*4*).

Before broader questions can be addressed using in vitro selection, it is necessary to explore some of the specific features displayed by many of the nucleic acid catalysts that have emerged from selection experiments, especially those that catalyze cleavage. For example, (a) Partial conversion. Many studies of individual nucleic acid catalysts report that their reaction goes only partially to completion. Hammerhead ribozymes, for example, are frequently reported to cleave only 40−60% at plateau (*5*−*6*). DNAzymes with ribonuclease activity similar to the ones studied here are also frequently reported with cleavage plateaus of 25−65% (*4*, *7*−*9*). The same is seen for DNAzymes with DNase activity (*10*). (b) Intra- versus intermolecular reactions. Many reactions catalyzed by nucleic acid catalysts are selected to be intramolecular, making the term "catalyst" technically incorrect; the catalyst is not regenerated. Many of the intramolecular reactions have analogous intermolecular processes that are truly catalytic, however, and these are often accessible both during the selection and in the subsequent kinetic analysis. (c) Loss of active catalysts during the setup. In many selection schemes, a library of catalysts must be synthesized and folded before the selection step begins. This leads to the possibility that the most active catalysts in a pool will be lost before the selection system can extract them. (d) Michaelis−Menten kinetic behavior. Many nucleic acid catalysts bind their substrate in a reversible step prior to the step where chemical bonds are made or broken. This should generate saturation kinetics similar to those seen in protein enzymes.

† This work was supported by the National Science Foundation Grant CHE-0213575 and the NASA Astrobiology Institute.

* To whom correspondence should be addressed. E-mail: mcarriga@ufl.edu (M.A.C.); sab@scinq.org (S.A.B.).

‡ Foundation for Applied Molecular Evolution, Inc. Telephone: (352) 271-7005.

§ University of Florida. Telephone: (352) 846-1980.

10.1021/bi049898l CCC: $27.50
Published on Web 08/18/2004

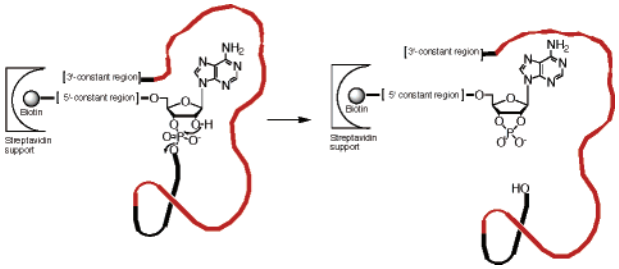

FIGURE 1: Library of DNA oligonucleotides containing an internal adenine riboside and a 40-nucleotide random region (represented in red) is attached to a solid support. The DNA-catalyzed ribonuclease reaction proceeds with the attack on the phosphorus electrophilic center by the ribonucleotide 2′-hydroxyl group, cleaving the phosphodiester backbone and releasing the catalytic portion of the DNAzyme from the solid support.

It is, of course, impossible to address these questions for the general reaction catalyzed by the general nucleic acid catalyst. Rather, such questions must be asked about individual nucleic acid catalysts effecting specific reactions. Such studies follow the tradition in physical organic chemistry, where detailed studies of many specific reactions eventually generate a body of literature that addresses broader issues in catalysis.

For this paper, we began with the work of Breaker and Joyce, who selected for DNA enzymes that catalyze the cleavage of a ribonucleotidyl-3′→5′-deoxyribonucleotide linkage in an oligodeoxyribonucleotide (*11*). The reaction almost certainly proceeds with the attack on the phosphorus electrophilic center via the ribonucleotide 2′-hydroxyl group (Figure 1). An adaptation of the Breaker−Joyce selection procedure led to several new catalysts for this reaction (Figure 2). One of these DNAzymes, designated **614**, was studied in detail to address some of the issues outlined above.

MATERIALS AND METHODS

Preparation of Precursor DNAzymes via Polymerase Chain Reaction (PCR)[1] *(12).* DNAzymes were prepared by PCR amplification of a template [synthesized by Integrated DNA Technologies (Coralville, IA) or from a clone] using a catalytic strand primer (*cat* + *ribose* or *cat* + *deoxyribose*, see Table 1) and a complementary strand primer (*compl*, *compl* + *5′P* or *compl* + *tail*). For trans-cleaving assays, DNAzymes were generated without the internal ribose using the *cat* + *deoxyribose* primer, identical to the *cat* + *ribose* primer except that the single ribo-adenosine in the *cat* + *ribose* was replaced with a 2′-deoxy*ribose*-adenosine. To obtain single-stranded catalysts, DNAzymes were produced using a catalytic strand primer and either a 5′-phosphorylated complementary strand primer (*compl* + *5′P*, for use with λ exonuclease) or a complementary strand primer with an 15-nucleotide polydeoxyriboadenosine tail appended to the 5′ via an 18-atom hexaethyleneglycol-based linker (*compl* + *tail*, for use in asymmetric PCR). This linker prevents polymerase read through. Templates all had the same 5′-constant region and 3′-constant region to which complementary and catalytic strand primers bind, separated by 40 nucleotides. *Ribose*-**614**, *deoxyribose*-**614**, and the library

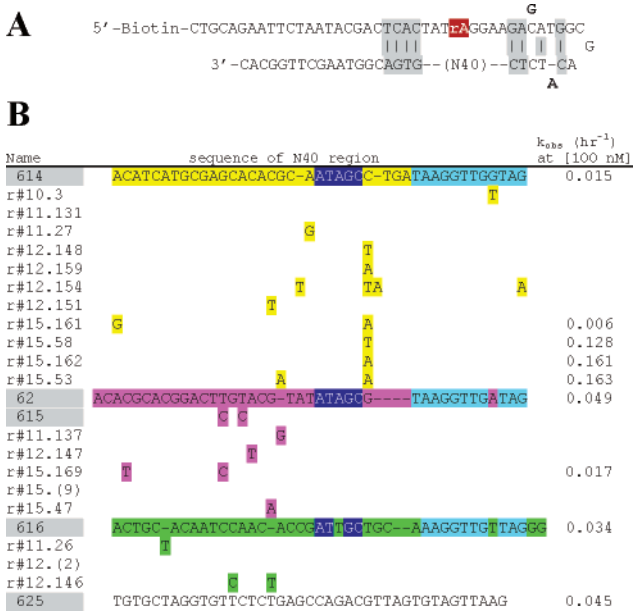

FIGURE 2: Sequence of the initial library and DNAzymes isolated from the in vitro selection. (A) The initial library was based on the sequence used by Breaker and Joyce (*11*) with an internal adenine riboside incorporated at position 28 to provide a cleavable linker. Two nucleotide substitutions were introduced to eliminate one of the clamps that were designed to hold the substrate and catalyst portions of the molecules in the library together. The original two nucleotides in the Breaker−Joyce sequence are shown in bold above and below the sequence used in this study. Base pairing that could form binding clamps are highlighted in gray. (B) DNAzymes isolated from multiple rounds of IVS. Sequences **614**, **62**/**615**, **616**, and **625** represent the major sequence classes initially cloned from the seventh round of the initial IVS. Sequences variants of these major classes were isolated from additional rounds of selection and are grouped according to sequence class (only variations from the prototype sequence are shown). Colored boxes are shown to highlight common motifs. Sequences isolated more than once are shown with the number of isolates identified in parentheses following the name.

templates were synthesized and polyacrylaminde gel electrophoresis (PAGE)-purified by Integrated DNA Technologies.

Typical conditions for a PCR contained up to 1 ng of template, 100 nM catalytic strand primer, 100 nM complementary strand primer, 100 μM deoxyribonucleotide triphosphates (dNTPs), 10 mM KCl, 20 mM Tris-HCl (pH 8.8), 10 mM $(NH_4)_2SO_4$, 2 mM $MgSO_4$, 0.1% Triton X-100, 3−4 units of polymerase (*Taq* or *Vent* exo-), and $\alpha[^{32}P]$CTP (10 μCi, for internally labeled samples), for a total volume of 100 μL. The PCR amplification cycle consisted of an initial incubation (3 min at 96 °C) followed by 20 PCR cycles of (45 s at 96 °C, 45 s at 50 °C, and 2 min at 72 °C).

PCR for in vitro selections (IVS) used *Vent* exo- polymerase (3−4 units) and excess catalytic strand primer (400 nM), with up to 40 cycles of PCR in the early rounds.

Preparation of Single-Stranded DNAzymes. Double-stranded DNAzymes generated via PCR with a 5′-phosphorylated complementary strand primer (*compl* + *5′P*) were converted to single-stranded DNA by digestion of the complementary strand using λ exonuclease (which is specific for the 5′-phosphorylated strand of double-stranded DNA). The DNA was recovered by EtOH precipitation, resuspended in exonuclease solution (25 μL; 5 units of λ exonuclease,

[1] Abreviations: dNTP, deoxyribonucleotide triphosphate; PCR, polymerase change reaction; PAGE, polyacrylaminde gel electrophoresis; IVS, in vitro selection.

Table 1: Name, Sequence, and Description of Oligonucleotides Used throughout This Paper

names used in text	description
ribose-**614**	5′-CTGCAGAATTCTAATACGACTCACTATRAGGAAGACATGGCGACTCTCACATC-ATGCGAGCACACGCAATAGCCTGATAAGGTTGGTAGTGACGGTAAGCTTGGCAC DNAzyme isolated from the in vitro selection in this study. It catalyzes the cleavage of the ribo-adenosine embedded within the *cat* + *ribose* primer, either as a part of its own sequence or in trans.
ribose-**614ΔC72T**	Mutant of *ribose*-**614** in which the cytosine at position 72 is replaced by a thymidine, resulting in a 30-fold lower rate of cleavage at 100 nM.
library template	5′-GTGCCAAGCTTACCGTCAC(N_{40})GAGATGTCGCCATCTCTTCC Complementary strand template containing a region of 40-nucleotide randomized region flanked on both sides with constant regions, one complementary to *cat* + *ribose* and the other identical to *compl*.
ribose-library	Random library generated by PCR amplification of the library template with *cat* + *ribose* and *compl* primers. Without selection, this library is predominately inactive. Selection of this library gave rise to DNAzyme **614** and others. All sequences contain the *cat* + *ribose* primer and therefore have the potential to function as substrates for **614** cleavage.
ribose-**lib62**	Individual clone isolated from a the *ribose*-library. This sequence has no intrinsic ribonuclease activity of its own but contains the *cat* + *ribose* primer and therefore can function as a substrate for **614** cleavage.
deoxyribose-**614**, *deoxyribose*-**lib62**, *deoxyribose*-**614ΔC72T**	Same sequences as *ribose*-**614,** *ribose*-**lib62,** and *ribose*-**614ΔC72T** but with the ribo-adenosine at position 28 replaced by a *deoxyribose*-adenosine (via PCR amplification with *cat* + *deoxyribose* primer). *Deoxyribose*-**614** is still capable of cleaving the ribo-adenosine embedded within the *cat* + *ribose* primer but only in trans.
compl-**614**	Complementary strand to *deoxyribose*-**614**.
cat + *ribose*	5′-CTGCAGAATTCTAATACGACTCACTATrAGGAAGACATGGCGACTCTC Primer used to generate full-length molecules from template, thus incorporating a ribo-adenosine (rA) at position 28. This oligo has no catalytic activity of its own and was therefore used as a substrate in trans cleavage assays.
cat + *deoxyribose*	Same oligonucleotide sequence as *cat* + *ribose* but with a deoxyribonucleotide replacing the rA. This primer was used to generate full-length DNAzymes without the ribo-adenosine moiety. DNAzymes incorporating *cat* + *deoxyribose* cannot be cleaved and therefore act as a true enzyme.
compl	5′-GTGCCAAGCTTACCGTCA This primer is complementary to the 3′ end of the catalytic strand of the full-length DNAzymes used in this study and is used to generate double-stranded DNAzymes via PCR.
compl + 5′P	This primer is the same sequence as the *compl* primer but with a phosphate attached to the 5′ position. This primer is used to generate double-stranded DNAzyme via PCR,followed by degradation of the complementary strand by λ exonuclease (an enzyme that specifically degrades 5′-phosphorylated DNA).
compl + tail	This primer is the same sequence as the *compl* primer but with a 15-nucleotide polyadenosine attached to the 5′ position via an 18-atom hexaethyleneglycol-based linker. Polymerase cannot efficiently read through this linker, so PCR using this primer genearates a double-stranded DNAzyme with a complementary strand that is 15 nucleotides longer than the catalytic strand, thus allowing purification of the catalytic strand via PAGE/urea.
chase	*cat* + *deoxyribose* oligo was used as the chase substrate for cleavage assays with **614** functioning as the enzyme.
28-nucleotide product	28-nucleotide product generated from cleavage of *ribose*-**614** (106 nucleotides).
78-nucleotide product	78-nucleotide product generated from cleavage of *ribose*-**614** (106 nucleotides).
cat nucleotides 29−45	5′-GGAAGACATGGCGACTCTC 5′-truncated version of *cat* + *deoxyribose* (containing nucleotides 29−45) used to generate double-stranded DNA of the 78-nucleotide *ribose*-**614** cleavage product for subsequent cloning.

67 mM glycine-KOH (pH 9.4), 2.5 mM $MgCl_2$, and 50 μg/mL BSA, for a PCR of 100 μL). Samples were mixed and incubated (30 min at 37 °C). Reactions were terminated with formamide stop dye (1 mg/mL xylene cyanol, 1 mg/mL bromophenol blue, and 10 mM EDTA, in 98% formamide) and heating (10 min at 80 °C). The single-stranded products were resolved by 8% PAGE/urea, and full-length single-stranded DNA products were excised. Gel slices of individual samples were crushed with individual disposable mortars and were eluted in buffer (350 μL; 500 mM NH_4OAc, 0.1 mM EDTA, and 0.1% SDS at pH 7) overnight. Gel-purified samples were extracted with phenol/$CHCl_3$/isoamyl alcohol (25:24:1) and then with $CHCl_3$/isoamyl alcohol (24:1), and the resulting DNA was precipitated in NH_4OAc and EtOH.

Single-stranded DNAzymes were also purified via asymmetric PCR using a complementary strand primer with a 15-nucleotide polydeoxyriboadenosine tail connected to the 5′-end of the primer by a C18 linker (*compl* + *tail*), at which *Vent* and *Taq* polymerases terminate. Complementary strand molecules generated by extension of a complementary strand primer containing the 5′ tail are longer than the full-length catalytic strand and were separated from the catalytic strand by PAGE/urea (8% acrylamide). Gel-purified samples were excised, extracted, and recovered as before.

5′-End Labeling of DNA. Single-stranded DNA (20 mM) was 5′-labeled with γ[^{32}P]ATP (20 μCi) using T4 polynucleotide kinase (10 units) in Tris-HCl buffer (70 mM at pH 7.6; 10 mM $MgCl_2$ and 5 mM dithiothreitol; final volume of 10 μL; for 30 min at 37 °C). An equal volume of TE was then added, and the mixture heated (20 min at 70 °C). End-labeled DNA was separated from unincorporated nucleotides by spinning through a G-25 column (600 g for 3 min).

DNAzyme Kinetic Assays. DNAzymes and substrates were isolated via EtOH precipitation and resuspended in HEPES buffer (50 mM at pH 7). Their concentration was estimated by Cherenkov counting. Samples were diluted to twice the desired final concentration with additional HEPES buffer. For trans assays, enzyme and substrates were typically mixed (unless otherwise noted) and diluted to twice the desired final concentration. Samples were then mixed with equal volume 2× reaction buffer (typically 2 M NaCl, 2 mM $MgCl_2$, and 50 mM HEPES at pH 7). Mixtures were then heated (96 °C for 3 min), and slowly cooled to 23 °C (over 10 min), collectively termed "slow cooling". The initial "time zero" point was the time at which the sample completed the slow cooling. Unless otherwise noted, reactions were run at 25 °C and terminated at various times by diluting an aliquot of the reaction into the formamide stop dye, followed by freezing (−20 °C). Samples were resolved using 8% PAGE/urea, and the product cleaved was quantified using a Bio-Rad phosphorimager. Data were analyzed using the GraphPad Prism 3.0a software package.

Cloning and Sequencing DNAzymes. Single-stranded DNAzymes were converted to duplex DNA by PCR amplification, usually with only the complementary strand primer *compl* (96 °C for 3 min; followed by 3 cycles of 45 s at 96 °C, 4 min ramp cool to 50 °C plus 45 s at 50 °C, and 1 min at 72 °C, followed by 7 min at 72 °C). When cloning cleaved and uncleaved **614**, the desired single-stranded DNA (either cleaved product or uncleaved reactant) was first isolated via PAGE/urea. PCR of the unpurified **614** reaction mixture containing both cleaved and uncleaved **614** with only *compl* primer yielded clones of only uncleaved **614** molecules; cleaved **614** molecules were therefore cloned by PCR amplifying gel-purified-cleaved fragments using the *compl* primer with the 5′-truncated catalytic primer *cat.nt29−45*. Fresh double-stranded PCR products were cloned using the TOPO TA Cloning System (InVitrogen) and plated on agarose plates containing ampicillin. Transformed cells were given only 15−30 min to recover in antibiotic-free media prior to plating on antibiotic-containing plates (to prevent recently transformed clones from doubling prior to plating, favoring isolation of only unique species from the original pool).

Clones were transformed into the TOPO TA Cloning Vector, and DNA was prepared from individual clones using the alkaline lysis protocol (*18*). Clones were sequenced using the *1224* plasmid sequencing primer (3.2 pM, 5′-CGCCAGGGTTTTCCCAGTCACGAC) with 300−500 ng of plasmid DNA template, 2× final concentration Big Dye reaction buffer, and 2 μL of Big Dye Terminator Sequencing mix in a final volume of 10 μL. Samples were overlaid with mineral oil and amplified by PCR (25 cycles, 96 °C for 30 s, 50 °C for 15 s, and 60 °C for 4 min). Sequencing samples were analyzed on an Applied Biosystems Prism 310 Genetic Analyzer. Sequencing results were confirmed by examining the chromatograms manually using the "Sequencher" software package.

In Vitro Selection. DNAzyme libraries for the first round of selection were prepared by a single cycle of runoff PCR using the library template (5′-GTGCCAAGCTTACCGTCAC-N_{40}-GAGATGTCGCCATCTCTTCC (where N indicates equal molar concentrations of A, T, G, and C) and *cat + ribose* primer. Runoff reactions volumes ranged from 3 to 20 mL, each containing 1 ng/μL library template, 100 nM catalytic strand primer, 100 μM dNTPs, 10 mM KCl, 20 mM Tris-HCl (pH 8.8), 10 mM $(NH_4)_2SO_4$, 2 mM Mg_2SO_4, 0.1% Triton X-100, 20 units/mL *Vent exo-*, and 4.3 μCi/mL α[^{32}P]CTP. Aliquots (1 mL) of each sample mixture (minus polymerase) were placed in Eppendorf tubes (1.5 mL), heated (96 °C for 8 min), and then slowly cooled to 55 °C over 30 min. Polymerase was added, and the samples were incubated (72 °C for 15 min). DNA was recovered by EtOH precipitation with NH_4OAc and glycogen as a carrier by storing overnight at −80 °C and then centrifuging in Corex tubes (16000*g* for 40 min at 4 °C). The EtOH was removed, and the pellet was resuspended in water (200 μL). DNA was recovered by precipitation a second time with EtOH (NH_4OAc) and centrifugation (16000*g* for 20 min at 4 °C). After the EtOH was removed, the pellet was resuspended in 1× binding buffer (1 M NaCl, 1 mM EDTA, and 50 mM HEPES at pH 7) and bound to a streptavidin column. The unbound material was removed by flushing the column with wash buffer (50 mM HEPES at pH 7). The complementary strand was removed by washing quickly with 0.2 M NaOH, followed again by the wash buffer. The cleavage reaction was initiated by eluting the wash buffer and replacing it with the reaction buffer (1 M NaCl, 1 mM $MgCl_2$, and 50 mM HEPES at pH 7). The cleaved products were eluted from the column after incubation for 2 h. The eluted material was used in a PCR with the *cat + ribose* and *compl + 5′P* primers to generate material for the next round of selection.

RESULTS

In Vitro Selection. An in vitro selection experiment to select for a DNAzyme having ribonuclease activity was conducted using a procedure adapted from Breaker and Joyce (*11*). A library was constructed containing a 5′-primer constant region and a substrate segment, which contained an internal ribo-adenosine at position 28. This was connected to a 3′-primer constant region by a segment, 40 nucleotides in length, having a random sequence. The 5′-constant region used by Breaker and Joyce was altered to minimize a base paired "clamp" engineered to favor association between the substrate and random portions (see Figure 2a) of the DNAzyme. Table 1 presents a summary of the many oligonucleotides discussed in this paper.

A cycle of selection and amplification was applied for 7 rounds to the library. A sampling of the DNA molecules recovered was then cloned and sequenced. Several DNA molecules having distinct sequences were isolated. When inspected for catalytic activity, the molecules cleaved themselves with apparent first-order rate constants ranging from 0.015 to 0.049 h^{-1} (Figure 2b). These rate constants are low in comparison to optimized DNAzymes obtained in the presence of divalent cation (ca. 60 h^{-1} Santoro and Joyce, in refs *12* and *13*, among others) but are comparable to Mg^{2+}-independent catalysts reported by Geyer and Sen (0.17 h^{-1}, in ref *7*) and by Faulhammer and Famulok (0.006−0.024 h^{-1}, in ref *8* and *9*). Additional rounds of selection isolated variants of the sequences initially identified in round 7.

The behavior of one catalyst, termed **614**, isolated from the seventh round of selection was examined. DNAzyme **614** was chemically synthesized and purified by PAGE by

Integrated DNA Technologies. Large quantities of internally radiolabeled **614** were generated by PCR using this **614** template. The catalytic strand of the double-stranded PCR products, termed *ribose*-**614**, was separated from its complement by two methods. In some cases, *ribose*-**614** was generated with a 5′-phosphorylated complementary strand primer (*compl* + *5′P*). After PCR, the complement was digested with λ exonuclease. Alternatively, *ribose*-**614** was generated using a complementary strand primer with a 15-nucleotide polyadenosine tail attached to its 5′ end via a PEG linker (*compl* + *tail*). The tail increased the length of only the complementary strand, allowing PAGE separation of the catalytic strand from its complement.

Purified *ribose*-**614** was resuspended in HEPES buffer, and cleavage reactions were initiated by adding an equal volume of 2× reaction buffer, immediate heating to 96 °C for 3 min, and slow cooling to 23 °C over 10 min (the setup). The reaction was then followed by gel electrophoresis. *Ribose*-**614** (100 nM) cleaves itself at a rate of 0.015 h^{-1}, which is slow in comparison to previously isolated DNazymes (*2*, *4*, *7*−*9*, *11*) but still significantly faster than the uncatalyzed reaction (Supplemental Figure 1 of the Supporting Information; the uncatalyzed cleavage rate is negligible in 300 h, as estimated from the cleavage of *ribose*-library shown in Supplemental Figure 2 of the Supporting Information).

*Cleavage of **614** Does Not Go To Completion.* A progress curve for *ribose*-**614** cleavage shows that the product formation ceased after ca. 65% conversion; this is a "cleavage plateau" (Supplemental Figure 1 of the Supporting Information). Such plateaus are frequently seen in selected DNAzymes and RNAzymes but are rarely explained. We considered six possible explanations for the failure of the cleavage reaction to go to completion. (1) The complementary strand may have been incompletely removed in the setup. This strand may inhibit the reaction or may erroneously increase the estimate of the uncleaved product if the radiolabeled complementary strand is assigned to the reactant. (2) Part of the substrate may be missing the adenine riboside that offers the cleavable site, because of failure in the synthesis of the *cat* + *ribose* primer. (3) The reaction might be reversible, with the 65% cleavage representing the achievement of the equilibrium between the uncleaved substrate and cleaved products. (4) The products of the reaction may inhibit **614**. (5) Part of **614** may adopt a conformation that is inactive. (6) Part of **614** might no longer have the correct sequence, having incurred a mutation during the synthesis of the template or amplification.

We examined each possibility.

Inhibition by Incompletely Removing the Complementary Strand Does Not Account for the Plateau. The complement of **614** (termed *compl*-**614**) was added in small amounts to *ribose*-**614** ([*ribose*-**614**] = 115 nM, and [*compl*-**614**] = 11.5 nM). The initial cleavage rate and plateau were unchanged (Supplemental Figure 1A of the Supporting Information). Similar results were seen at a lower concentration of *ribose*-**614** (11.5 nM) plus *compl*-**614** (1.15 nM). Experiments with equal amounts of *ribose*-**614** (200 nM) and *compl*-**614** (200 nM) found that the plateau was dramatically lower (Supplemental Figure 1B of the Supporting Information), even though the initial cleavage rate was unchanged. Similar results were seen with *ribose*-**614** at 50 nM plus *compl*-**614** at 50 nM. This showed that the complementary strand inhibited cleavage by **614** and the importance of removing the complementary strand prior to measurement of DNAzyme kinetics.

We then asked whether the presence of the complementary strand could explain the incomplete cleavage of *ribose*-**614**. Two independent procedures (exonuclease digestion and asymmetric PCR) were used to generate *ribose*-**614** lacking its complement. Experiments with each yielded approximately the same cleavage plateau. This suggested that the plateau is not the consequence of incomplete removal of *compl*-**614**, because it is unlikely that the amounts of complement remaining following the two procedures are the same. In fact, it is difficult to imagine that any *compl*-**614** remains following the purification using the asymmetric PCR procedure, because the complementary strand is 15-nucleotides longer than the catalytic strand and would almost certainly be removed by PAGE purification.

To assess the amount of complementary strand remaining after exonuclease treatment, we treated *ribose*-**614** generated via the exonuclease method with base (0.5 M NaOH at 80 °C for 1 h). This cleaves all of the substrate at the adenine riboside site. The amount of cleaved products was similar to that with the 5′-^{32}P-labeled *cat* + *ribose* primer (85−95% cleaved for *ribose*-**614** versus 90−97% cleaved for *cat* + *ribose* primer following treatment with base). The incomplete cleavage of *cat* + *ribose* primer by base suggest a lack of chemical susceptibility of the primer (discussed below). Because contamination from the complementary strand cannot be present in the *cat* + *ribose* primer, the ca. 5% difference between base cleavage of the *cat* + *ribose* primer and the full-length *ribose*-**614** is an estimate of the upper limit of the amount of complementary strand that might remain from incomplete degradation by exonuclease.

The efficiency with which λ exonuclease removes the complementary strand was also tested using a 5′-^{32}P-labeled *cat* + *ribose* primer to synthesize full-length, double-stranded *ribose*-**614** without 5′ phosphate on the complementary strand primer. The duplex PCR product was divided into two aliquots. One was subjected to standard exonuclease treatment, while the other sample was untreated. The samples were resolved by PAGE/urea to determine the amount of full-length product. Less than 10% of the original phosphorylated strand (compared to that of the untreated sample) remained following exonuclease digest. These results rule out contamination by residual *compl*-**614** as a major cause of incomplete **614** cleavage.

An Approach to Chemical Equilibrium Does Not Account for the Plateau. The failure of a substrate to be completely transformed to the product may result from an approach to chemical equilibrium between substrates and products in a reversible reaction. To test for this, *ribose*-**614** (200 nM) was incubated for 144 h. At this time, the plateau had been reached and the reaction mixture was divided into three aliquots. One aliquot was reserved. The second was diluted 25-fold with reaction buffer. Diluting is expected to drive the equilibrium toward the cleaved product, assuming the products dissociate following cleavage (multiple turnover experiments described later validate this assumption).

An equal amount of a variant of *ribose*-**614**, *deoxyribose*-**614**, was added to the third aliquot. The compound *deoxyribose*-**614** is the same sequence as *ribose*-**614** but with an

uncleavable adenine 2′ deoxyriboside replacing the cleavable adenine riboside at position 28. As discussed below, *deoxyribose*-**614** is a true catalyst, acting in trans. Its addition in excess to *ribose*-**614** ensured that catalytic activity was sufficient to see cleavage at the plateau if it was occurring. Neither treatment significantly altered the plateau (data not shown), excluding reversibility as its explanation.

In a second experiment, the 78-nucleotide product of *ribose*-**614** cleavage was isolated via gel purification. This product was radiolabeled and, following gel purification, incubated (in excess) with full-length *ribose*-**614** (unlabeled). As the unlabeled *ribose*-**614** becomes cleaved and if the reverse reaction ligation occurs, excess of the 78-nucleotide product ensures that it may capture by ligation the 28-nucleotide product, converting the 78-nucleotide product to full-length *ribose*-**614** over time. The reaction was monitored for 400 h. No conversion of the 78-nucleotide product to full-length material was observed (data not shown). This also excludes reversibility as an explanation for the plateau.

Testing if the Cleavage Products Are Acting as Catalysts or Inhibitors. By incorporating a short self-complementary segment that encourages a hairpin to clamp together the substrate and catalytic portions of the DNAzyme, Breaker and Joyce hoped to increase the chance that their library would contain molecules that self-cleave rapidly in cis. Further, cis cleavage might be expected to predominate over trans cleavage, because the substrate is covalently bonded to the catalyst. The possibility that either cleaved product continues to act as a ribonuclease in trans or as an inhibitor cannot be ruled out. This is especially true for **614**, where the clamp that might favor a hairpin and therefore cis cleavage is not present.

To test this, the 28- and 78-nucleotide products were gel-purified. These products were added in equal amounts to a sample of uncleaved *ribose*-**614**. Cleavage of *ribose*-**614** occurred at the same rate in the presence or absence of the 28- and 78-nucleotide products (Supplemental Figure 2 of the Supporting Information). This suggests that 28- and 78-nucleotide products do not act as inhibitors or catalysts, at least when both are present in stoichiometric amounts (approximately the highest concentration they reach under normal **614** cleavage conditions).

The 28- and 78-nucleotide products were also added to a sample of the *ribose*-library used in the selection. The *ribose*-library contains the *cat* + *ribose* primer followed by a segment of random sequence. Thus, it contains substrates that are (for the most part) not catalysts and serves as the opposite of *deoxyribose*-**614**, which is a catalyst but not a substrate. The *ribose*-library alone does self-cleave to a detectable extent, as expected, given that an unselected, random library has very few active catalysts.

The 28-nucleotide product alone did not cleave *ribose*-library, showing that this product is not a catalyst. The 78-nucleotide product alone did cleave *ribose*-library, although with a very low rate constant ($k_{obs} = 0.0006\ h^{-1}$, 35-fold lower than *ribose*-**614** under similar conditions). The 28-nucleotide product with the 78-nucleotide product reduced cleavage of the *ribose*-library below that observed with the 78-nucleotide product alone. This inhibition is presumably because the 28-nucleotide product competes with the *ribose*-library substrate in binding to the 78-nucleotide catalyst. Inhibition of **614** by the 28-nucleotide product is not noticeable presumably because the 28-nucleotide product does not compete as effectively for **614** as does a second molecule of **614**.

*Improperly Folded Ribose-**614** Accounts for Part of the Plateau.* We then asked whether *ribose*-**614** folds into active and inactive conformations, with the inactive form contributing to the cleavage plateau. Predictions of the conformation of *ribose*-**614** using Mfold (version 3.1, see ref *15*) showed several potential structures. Close inspection of *ribose*-**614** on a nondenaturing gel suggested that two bands were present in the starting material, one converting to a third band upon incubation under reaction conditions and the other remaining unchanged. This is consistent with the hypothesis that *ribose*-**614** adopts active and inactive conformations.

To test this, *ribose*-**614** was incubated until the plateau was reached (140 h). The mixture then was diluted into 2 volumes of formamide and heated (90 °C for 2 min). The uncleaved *ribose*-**614** was purified by PAGE/urea, resuspended in buffer, refolded using the slow cooling protocol, and subjected to cleavage conditions a second time. An additional 25% of the *ribose*-**614** sample was cleaved in the 300 h following gel purification (Supplemental Figure 3 of the Supporting Information). This additional cleavage following gel purification suggests that some of the initially uncleaved *ribose*-**614** was in an inactive conformation. It is notable, however, that the gel-purified *ribose*-**614** reached a plateau of ca. 25%, significantly lower than the cleavage plateau of the original sample.

If misfolding was the only cause of incomplete cleavage, a plateau of approximately 65% would be expected in the second round of cleavage. The fact that the gel-purified sample reaches a lower plateau indicates that misfolding may account for only ca. 9% of total uncleaved fraction in the original sample (because an additional 25% of the sample was cleaved following gel purification and ca. 35% of the original sample remains uncleaved, the fraction of the initial sample that is misfolded is 25% of 35% or 9%).

We considered the possibility that gel purification removed an inhibitor of cleavage. *Ribose*-**614** was incubated to reach the plateau (141 h), and an aliquot was heated and slowly cooled. Any molecule in an inactive conformation was thus given another chance to adopt an active conformation. As in the gel-purification experiments, denaturing and refolding via this procedure increase the amount of material cleaved (Supplemental Figure 4 of the Supporting Information). The cleavage plateau over the first 150 h following reheating is about 10% higher than the untreated sample (in agreement with the estimate of 9% above) but still well below the ca. 90% cleavage when treated by strong base. When untreated samples are incubated beyond 300 h, the cleavage levels approach those seen when samples are reheated at 140 h, suggesting that refolding into active conformations may occur slowly at room temperature. Thus, alternative conformations account for some but not all of the plateau seen between 150 and 300 h.

*Mutations Introduced into **614** during Cloning and Sequencing Account for Part of the Plateau.* The ability of the base to cleave ca. 94% of the *cat* + *ribose* primer suggests that about 6% of the *cat* + *ribose* primer and therefore any full-length DNAzyme made from the *cat* + *ribose* primer may be missing the adenine riboside unit that is the site for

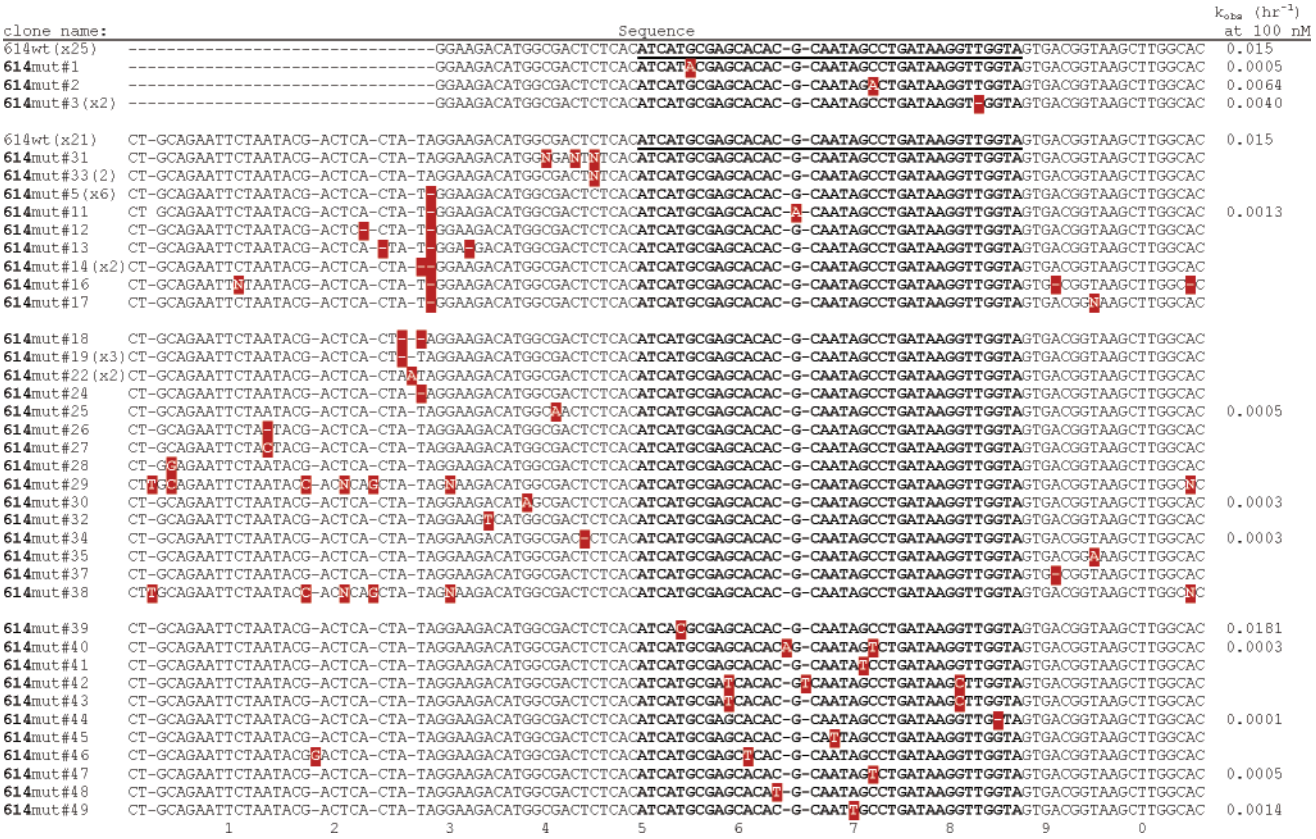

FIGURE 3: Sequence alignment of cleaved and uncleaved cloned **614** sequence variants. Mutations of **614** are highlighted in yellow; "N_{40}" region between primers is bold in each sequence and underlined in the original (no mutation) **614** sequence. Apparent first-order catalytic rate constants (at 100 nM, in units of per hour) are shown to the right for a sample of mutant-**614** DNAzymes.

cleavage. Other sequence variants may be present throughout *ribose*-**614** as well, either as a result of mutations introduced during the synthesis of the primers and template or as mutations introduced by the polymerase during PCR. These mutations may reduce or eliminate the catalytic power of a fraction of the *ribose*-**614** DNAzyme pool.

This possibility was examined by cloning and sequencing DNA molecules from the cleaved and uncleaved fractions of *ribose*-**614** after the plateau had been reached (Figure 3). Of the 29 sequenced clones of the 78-nucleotide-cleaved product of *ribose*-**614**, only 4 (14%) were found to be mutants. The mutations, at 3 sites, were in the N_{40} region between the primers.

In contrast, of the 66 clones from the portion of *ribose*-**614** that remained uncleaved at the plateau, only 64% had at least 1 mutation (42 individuals). Some 18% had a mutation in the N_{40} region; 5% had a mutation in the complementary strand primer; and 48% had a mutation in the catalytic strand primer (including 20% of the uncleaved *ribose*-**614** molecules sampled that were missing the adenine riboside cleavable site). Excluding molecules missing the adenine riboside cleavable site, 44% of the uncleaved molecules possessed a mutation. This corresponds to 15% of the total initial population (44% of ca. 35% of the total initial population remaining uncleaved at the plateau).

The extent of misfolding in **614** was estimated by assuming that all unmutated sequences from the uncleaved pool at the plateau remained uncleaved because they had adopted an inactive conformation. When given this information, 13% of the total population is calculated to be misfolded (36% of the unreacted material is not mutated, and the unreacted material at the plateau is ca. 35% of the total). This is consistent with the estimate above based on the outcome of a cycle of unfolding and refolding.

Several of the **614** mutants were tested to see if the mutations in fact reduced the rate of self-cleavage. A total of 11 of the 12 **614** mutants that were tested showed cleavage rates reduced by 10−100-fold compared to *ribose*-**614** (Figure 3).

*Ribose-**614** Catalysis is not Mg^{2+}-Dependent.* The mono- and divalent cation requirements for *ribose*-**614** activity were then examined. Reducing the concentration of NaCl from 1 to 0.1 M eliminated cleavage. Only a modest change in the rate of cleavage of *ribose*-**614** (100 nM) was observed when the reaction was run in the absence of $MgCl_2$ (with and without 1 mM EDTA, initial rate of 1.32×10^{-2} and 1.37×10^{-2} h^{-1}, respectively) or in the presence of $MgCl_2$ (1 mM, 1.53×10^{-2} h^{-1}; 10 mM, 1.70×10^{-2} h^{-1}; or 100 mM, 2.52×10^{-2} h^{-1}). Catalysis by **614** therefore does not require Mg^{2+}, even though **614** was selected in the presence of $MgCl_2$ (1 mM). The rates of two other catalysts isolated from this selection (*ribose*-**62** and *ribose*-**616**) were also largely unchanged when the $MgCl_2$ (1 mM) of the reaction buffer was replaced with EDTA (1 mM). For *ribose*-**625**, another molecule isolated from the selection, cleavage was eliminated by replacement of $MgCl_2$ by EDTA at 25 °C.

*Ribose-**614** Cleaves in Trans.* A series of experiments was then performed to examine the rate of cleavage as a function of the concentration. Self-cleavage is expected to be kinetically first order. Cleavage in trans is expected to be kinetically second order, meaning that an apparent first-order rate constant k_{obs} will not be independent of [DNAzyme]

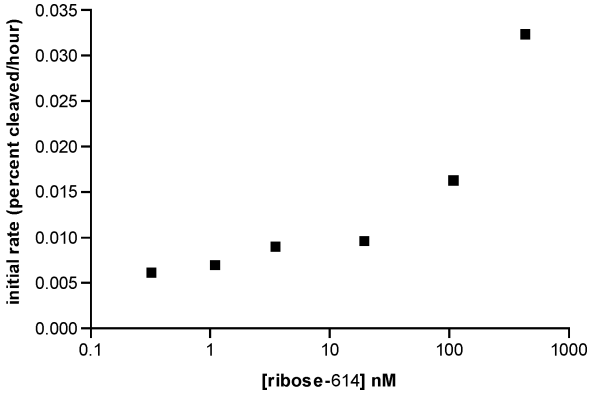

FIGURE 4: Initial rate of *ribose*-**614** cleavage as a function of [*ribose*-**614**]. At higher concentrations, a second-order process is apparent. The rate constant for the apparent first-order process (uncorrected for the cleavage plateau), from the *y* intercept, is ca. 0.006 h^{-1}. Primary data are in the Supporting Information.

Table 2: Data from Plot $\ln[S]_t$ versus Time for *Ribose*-**614** Cleavage at Various Concentrations Fit to a Linear Equation

[*ribose*-**614**] (nM)	430	108	19.4	3.5	1.1	0.3
−(slope of $\ln[S]_t$)	0.0032	0.0035	0.0030	0.0031	0.0030	0.0042
R^2	0.78	0.89	0.92	0.90	0.97	0.97

and fall to zero as [DNAzyme] falls to zero. A convenient way to separate simultaneous intra- and intermolecular processes is to plot the apparent k_{obs} as a function of [DNAzyme]. The *y* intercept is k_{uni} for the unimolecular reaction, while the slope of the line (with a nonzero slope) reflects a second-order process.

Figure 4 shows a plot of the apparent k_{obs} versus [*ribose*-**614**]; primary cleavage profiles are shown in Supplemental Figure 5 of the Supporting Information. At [*ribose*-**614**] below 20 nM, the rate is independent of [*ribose*-**614**]. At higher concentrations, however, the apparent k_{obs} increases with increasing [*ribose*-**614**]. These results are consistent with a model that includes both uni- and bimolecular processes (the linear region for [*ribose*-**614**] below 20 nM is predominately unimolecular, while the linear region for [*ribose*-**614**] greater than 20 nM is predominately bimolecular). A best-fit line extrapolated to infinite dilution for [*ribose*-**614**] below 20 nM gives an intercept corresponding to a unimolecular rate constant of 0.006 h^{-1}. This is an underestimate because the rate constant, based on initial rates, is uncorrected for the cleavage plateau (see below). An alternative way to obtain a rate constant for a first-order process plots the log of uncleaved [*ribose*-**614**] (substrate remaining) versus time. Here, the progress of cleavage at low [*ribose*-**614**] fit a linear model well, while the progress at higher concentrations did not (Table 2). This suggests that, below 20 nM, a unimolecular rate process dominates, while a bimolecular rate process contributes above 20 nM. The rate constant estimated in this manner for [*ribose*-**614**] at 0.3 nM was 0.0042 h^{-1} (uncorrected for the plateau), in good agreement with the estimate above.

We then asked if the progress curve for cleavage at high and low [*ribose*-**614**] fit best to a single exponential (in which both the rate and plateau can vary) or the sum of two exponential equations (in which both the rate and plateau can vary for each of the two equations). At *ribose*-**614** concentrations ≤ 3.5 nM, progress curves fit best to a single exponential. At higher concentrations, the progress curve is

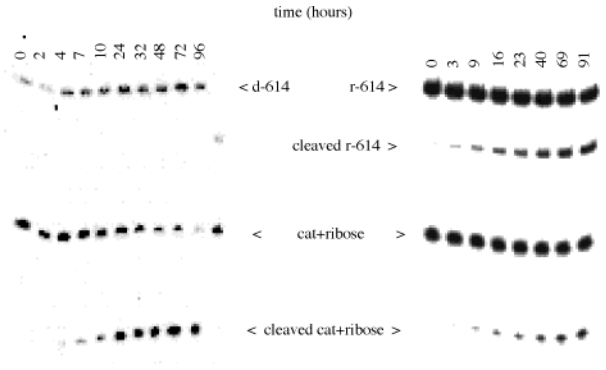

FIGURE 5: Both *deoxyribose*-**614** (left panel) and *ribose*-**614** (right panel) cleave *cat* + *ribose* primer in trans. Internally labeled *deoxyribose*-**614** (100 nM) or *ribose*-**614** (100 nM) were mixed with 5′-end-labeled *cat* + *ribose* (100 nM) and incubated under reaction conditions. The *deoxyribose*-**614** does not contain the riboadenosine and therefore does not cleave itself. Unless otherwise stated, all kinetics were performed under standard reaction conditions, namely, 1 M NaCl, 1 mM $MgCl_2$, and 50 mM HEPES at 25 °C, and errors in percent cleaved are ≤ ±2 percentage points.

fit best by the sum of two independent exponentials. This suggests that a single process dominates transformation of *ribose*-**614** at low concentrations. (As seen in Supplemental Figure 5 of the Supporting Information, a single-exponential curve does not fit well to cleavage data when [*ribose*-**614**] is 430 nM; presumably this is because two reaction mechanisms, one in cis and one in trans, are occurring simultaneously and with substantially different rates. Because the data fit poorly to a single-exponential curve, such estimates misrepresent the cleavage plateau and rate constants. Rate constants are therefore also estimated from the linear portion of the progress curve, focusing on the faster of the two mechanisms.)

If multiple active conformers exist at low [*ribose*-**614**], they are either in rapid equilibrium or self-cleave with comparable rate constants. The first-order constant was then corrected given information collected above about the plateau. After correction, a single-exponential curve fit to the progress curve for 0.3 nM *ribose*-**614** cleavage under unimolecular conditions. A k_{uni} of 0.011 h^{-1} was estimated (with a plateau of 61%).

*Various Ribose-Containing Substrates Are Cleaved by Deoxyribose-**614**.* To establish trans cleavage in this system, internally labeled *ribose*-**614** (which yields the 78-nucleotide fragment as the only labeled product) was incubated with 5′-^{32}P-labeled *cat* + *ribose* primer (100 nM). The *cat* + *ribose* contains the substrate domain of *ribose*-**614** but is not catalytically active. Here, *cat* + *ribose* is cleaved, as is *ribose*-**614** (right panel of Figure 5). This establishes trans cleavage by *ribose*-**614**. The cleavage of *ribose*-**614** (100 nM) in the presence of *cat* + *ribose* primer (100 nM) was lower than *ribose*-**614** incubated alone (at 100 nM), suggesting that the *cat* + *ribose* primer competes with *ribose*-**614** for trans cleavage by *ribose*-**614** (Supplemental Figure 6 of the Supporting Information).

Trans cleavage was also tested by challenging *deoxyribose*-**614** (a modified form of *ribose*-**614** in which the adenine riboside was replaced by a noncleavable deoxyadenosine) with various substrates, each containing the *cat* + *ribose* sequence. These included (a) the *cat* + *ribose* primer, (b) a pool of molecules incorporating the *cat* + *ribose*

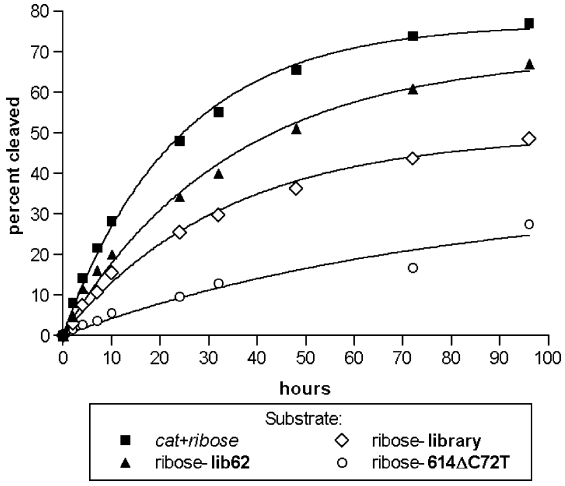

FIGURE 6: Compound *deoxyribose*-**614** can cleave various substrates in trans. Unlabeled *deoxyribose*-**614** (270 nM) was incubated with various radiolabeled substrates (*cat* + *ribose*, ■; *ribose*-**lib6lo2**, ▲; *ribose*-library, ◇; or *ribose*-**614ΔC72T**, ○) each at 7.5 nM. Each substrate possessed the same 5′-primer sequence containing the adenine riboside. Compound *deoxyribose*-**614** does not cleave itself, and the percentage cleaved is the fraction of the substrate converted to product. Data are fit to a first-order exponential curve. Errors in the measurement of radioactivity depend on the amounts of radioactivity being counted, of course, but are ca. ±20% (in percent, not percentage points) for the weakest bands when measured by the phosphorimager. That is, for a point that reflects 2% cleavage, the uncertainty in the value is captured by the statement that the number of counts ranges from 1.6 to 2.4% cleavage. For points that reflect close to 80% cleavage, the uncertainty is ca. ±2% and thus is captured by the statement that the number of counts ranges from 78 to 82% cleavage. As an approximation, one can regard the data reported in this and other figures as being accurate to ≤ ±2 percentage points. Errors in the measurement of time are ±1 min.

primer followed by a random region and a 18-nucleotide constant region (*ribose*-library), which collectively have no detectable catalytic activity, (c) a single clone from the *ribose*-library, (*ribose*-**lib62**), which also has no detectable catalytic activity, and (d) a mutant of **614** (**614ΔC72T**) that has ca. 30-fold reduced activity compared to **614**, at 100 nM.

Each substrate was cleaved by *deoxyribose*-**614** (Figure 6) although with different efficiencies (*deoxyribose*-**614** cleavage of *cat* + *ribose* is also shown in the left panel of Figure 5). *Ribose*-**614ΔC72T** (which should fold like *ribose*-**614**) is cleaved by *deoxyribose*-**614** more slowly (suggesting that *ribose*-**614ΔC72T** may fold so as to make the substrate domain inaccessible to catalysts), while the *cat* + *ribose* primer is cleaved faster. The fact that the small *cat* + *ribose* primer is better than full-length substrates is consistent with the view that folding in longer substrates inhibits trans cleavage by *deoxyribose*-**614**. The uni- and bimolecular mechanisms by which **614** can cleave are summarized in Scheme 1.

Competition Studies of Ribose-614 Cleavage. We then tested the ability of three of the above substrates, each with their ribose replaced by 2′-deoxyribose (*cat* + *deoxyribose* primer, *deoxyribose*-**614ΔC72T**, and *deoxyribose*-**lib62**), to compete with *ribose*-**614** for self-cleavage. These competitors were added in 9-fold excess over *ribose*-**614**. For comparison, 9-fold excess of *deoxyribose*-**614** was added to *ribose*-**614**.

The addition of *deoxyribose*-**614** (270 nM) to *ribose*-**614** (30 nM) increased the rate of *ribose*-**614** cleavage to the same

Scheme 1: **614** Can Cleave via a Uni- and Bimolecular Mechanism

Unimolecular Kinetic Scheme:

$$614_{unfolded} \underset{k_{-1\,(uni)}}{\overset{k_{1\,(uni)}}{\rightleftharpoons}} 614_{folded} \xrightarrow{k_{cat\,(uni)}} Products$$

Bimolecular Kinetic Scheme:

$$E + S \underset{k_{-1\,(bi)}}{\overset{k_{1\,(bi)}}{\rightleftharpoons}} E{\cdot}S \xrightarrow{k_{cat\,(bi)}} E{\cdot}P$$

E = *ribose*-**614** or *deoxyribose*-**614**
S = *ribose*-**614**, *ribose*-**lib62** or *cat*+*ribose*

level as seen for *ribose*-**614** at 300 nM (Supplemental Figure 7 of the Supporting Information). The cleavage of *ribose*-**614**, however, was reduced by excess *cat* + *deoxyribose* or *deoxyribose*-**lib62**. This showed that these molecules compete for *ribose*-**614** self-cleavage.

Curiously, addition of a 9-fold excess of *deoxyribose*-**614ΔC72T** to *ribose*-**614** did not reduce the rate of *ribose*-**614** cleavage but rather increased it. The ability of *deoxyribose*-**614ΔC72T** to cleave *ribose*-**614** may indicate that the mutation alters the ability of *deoxyribose*-**614ΔC72T** to function as a substrate without inactivating its catalytic domain, consistent with the observation above that *ribose*-**614ΔC72T** is itself a poor substrate for *deoxyribose*-**614** cleavage.

The competition study above was done at high [*ribose*-**614**] to favor trans cleavage. A parallel study at low concentrations of *ribose*-**614** (favoring unimolecular cleavage) showed no inhibition of *ribose*-**614** self-cleavage by *deoxyribose*-**lib62** competitor (Supplemental Figure 8 of the Supporting Information).

Saturation Kinetics in Trans Cleavage by Deoxyribose-614. Two mechanisms for the trans bimolecular reaction were considered. In the first, *deoxyribose*-**614** cleaves its substrate on every encounter. This gives a linear slope in a plot of an apparent rate constant versus [catalyst] or [substrate] over the entire concentration range.

An alternative second-order process is possible, however. Here, the substrate and catalyst form a complex that can dissociate before it reacts. This gives saturation Michaelis−Menten kinetics.

To search for saturation kinetics, we exploited *deoxyribose*-**614** as a DNAzyme that cannot act upon itself but must act in trans. Concentrations of *deoxyribose*-**614** were scanned to find a range where the apparent second-order rate constant reaches a plateau reflecting saturation. Various substrates were used, including *cat* + *ribose*, *ribose*-**lib62**, and *ribose*-**614**, at low amounts relative to *deoxyribose*-**614** (Supplemental Figure 9 of the Supporting Information; primary cleavage profiles are in Supplemental Figure 10 of the Supporting Information). Cleavage rates did not increase (2000−6000 nM *deoxyribose*-**614**), suggesting saturation of the bimolecular process.

Fitting the cleavage data to a modified Michaelis−Menton equation ($Y = V_{max}$[DNAzyme]/(K_d + [DNAzyme]) gave a dissociation constant (K_d) of 29.0, 37.3, and 25.5 nM for *cat* + *ribose* primer, *ribose*-**614**, and *ribose*-**lib62** substrates, respectively (this assumes that unbinding is fast compared to the reaction). The $k_{cat(bi)}$, determined from the maximum rate of cleavage with the saturating enzyme, was 0.056, 0.048, and 0.049 h^{-1} for *cat* + *ribose*, *ribose*-**614**, and *ribose*-**lib62** substrates, respectively. Further data are shown in Supplemental Figure 11 of the Supporting Information.

*Compound Deoxyribose-**614** Cleaves with Multiple Turnovers.* To show that *deoxyribose*-**614** catalyzes cleavage with multiple turnovers, either the *cat* + *ribose* or *ribose*-**lib62** substrate was incubated in a 4-fold excess over *deoxyribose*-**614** (133:33 and 400:100 nM substrate/enzyme) (Supplemental Figure 12 of the Supporting Information). With 400 nM enzyme and 100 nM substrate, two turnovers of substrate were observed at 100 h for the *cat* + *ribose* substrate and 200 h for the *ribose*-**lib62** substrate.

As seen under single-turnover conditions, the *cat* + *ribose* substrate is cleaved faster under multiple-turnover conditions than the full-length *ribose*-**lib62** substrate (at equivalent concentrations). This may be attributable to a better ability of the *cat* + *ribose* substrate to bind with or dissociate from the enzyme or a lower proclivity for forming nonproductive interactions.

Catalytic Power in Trans Is Unaffected by Annealing Protocol. The impact of the slow cooling protocol on trans cleavage was tested by mixing *deoxyribose*-**614** with the substrate (*ribose*-**lib62** or *cat* + *ribose*) either before or immediately after the slow cooling. This change in the annealing procedure did not noticeably alter the cleavage profile (Supplemental Figure 12 of the Supporting Information).

At high concentrations (200 nM), the rate of cleavage of *ribose*-**614** was unchanged by omitting the slow cooling (Supplemental Figure 13a of the Supporting Information). This also shows that intermolecular folding at the start of the reaction is not significantly effected by the annealing protocol, even though denaturation by heating allows molecules in inactive conformations to refold into active conformations (Supplemental Figure 4 of the Supporting Information). Similar experiments at low [*ribose*-**614**] favoring cis cleavage showed a slight decrease in initial rate with the omission of slow cooling (Supplemental Figure 13b of the Supporting Information).

*Commitment Step for Deoxyribose-**614** Cleavage.* If the rate-limiting step is the dissociation of the product−enzyme complex, a burst is expected in the initial phase of multiple turnover kinetics. To seek a burst, the concentration of *deoxyribose*-**614** as a catalyst was held constant at 20 nM, while the concentration of *cat* + *ribose* as a substrate was varied from 100 to 2000 nM (Supplemental Figure 14 of the Supporting Information). Turnover of the substrate to product remained linear well beyond the initial turnover for all substrate concentrations, revealing no burst phase and suggesting that the overall rate is not limited by DNAzyme·product dissociation.

To estimate the relative magnitudes of $k_{cat(bi)}$ and $k_{-1(bi)}$, a chase was performed with unlabeled *cat* + *deoxyribose* added after 4 h. The *cat* + *deoxyribose* chase is a substrate analogue that cannot be cleaved and therefore should compete with the labeled substrate. If all of the substrate−catalyst complex proceeds to product (which is the case if $k_{cat(bi)} \gg k_{-1(bi)}$), then addition of the unlabeled chase will not influence the subsequent rate of appearance of labeled products. If, however, the rate of substrate dissociation from the catalyst is faster than cleavage ($k_{cat(bi)} \ll k_{-1(bi)}$), then unlabeled chase molecules lacking a cleavable site should consume the newly disassociated catalyst and the production of labeled products should largely cease.

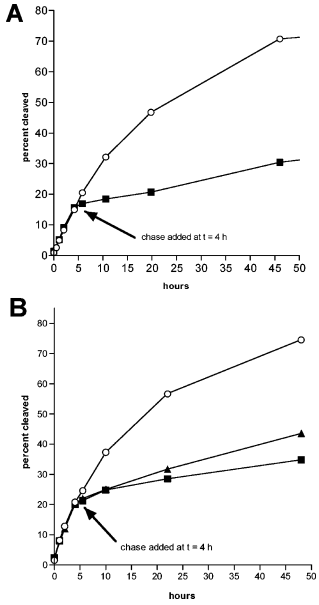

FIGURE 7: Cleavage of various substrates by **614** is reduced by the addition of unlabeled chase, indicating that the rate of E·S dissociation is faster than the chemical step of cleavage. (A) Saturating amounts of *deoxyribose*-**614** (2 μM) cleaving *ribose*-**614** (4 nM), with (■) and without (○) chase (10 μM) added at 4 h. (B) Saturating amounts of *deoxyribose*-**614** (2 μM) cleaving *ribose*-**lib62** (4 nM), without chase (○) and with chase (5 μM, ▲; or 10 μM, ■) added at 4 h.

In the chase, *deoxyribose*-**614** enzyme (2 mM, saturating) acted in trans on small amounts (4 nM) of *ribose*-**614** substrate. When the *cat* + *deoxyribose* chase was present at a 5-fold excess over the enzyme (10 mM added at $t = 4$ h), a decrease in the rate of cleavage of *ribose*-**614** after addition of the chase was observed (Figure 7a). The cleavage levels of *ribose*-**614** following the addition of chase is reduced below that seen for a predominately cis cleavage reaction of 1.1 nM *ribose*-**614** (Supplemental Figure 15 of the Supporting Information). This suggests that $k_{cat(bi)} \ll k_{-1(bi)}$.

Similar results were seen following the addition of chase to *ribose*-**614** under trans cleavage conditions (data not shown). Cleavage of *ribose*-**614**, however, was not completely eliminated by the chase. This suggested several explanations, including the persistence of cis cleavage in the presence of chase or insufficient chase. Chase experiments conducted with *ribose*-**614** cleaving in cis (2 nM) showed no significant change in cleavage following the addition of 30 nM chase (data not shown).

If $k_{cat(bi)} \ll k_{-1(bi)}$, the enzyme−substrate complex will dissociate to give reactants more rapidly than it will form products. If association is also relatively rapid, however, with insufficient chase, the enzyme may bind and release a number of chase molecules until it finds a labeled substrate. The reduction in cleavage should therefore depend on the relative amounts of chase, enzyme, and substrate molecules.

To test this directly and without self-cleavage, chase experiments were performed with saturating levels of *deoxyribose*-**614** enzyme (2 mM**)** cleaving *cat* + *ribose* substrate (4 nM) and chase in either 5 or 10 mM. Cleavage is greatly reduced, but not eliminated, following the addition of the chase (Figure 7b). The reduction of cleavage was slightly greater with chase in 5-fold excess over the enzyme as compared to only a 2.5-fold excess. Together, these experi-

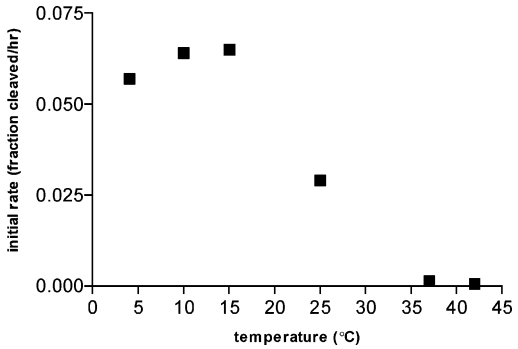

FIGURE 8: *Ribose*-**614** rate of self-cleavage in trans is increased at lower temperatures. *Ribose*-**614** (200 nM) was incubated at various temperatures from 4 to 42 °C. Initial rates were calculated and plotted versus temperature.

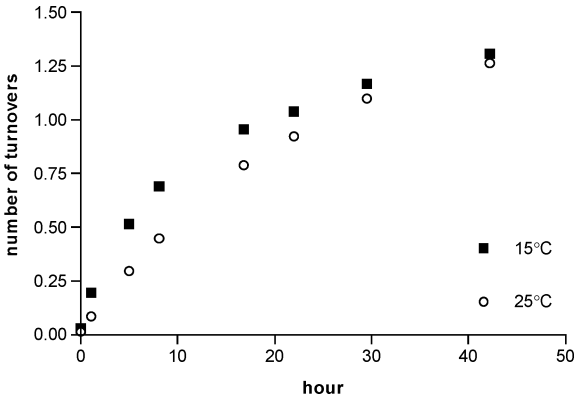

FIGURE 9: Burst kinetics (a higher cleavage rate during the first turnover compared to subsequent turnovers) is enhanced at lower temperatures. *Ribose*-**lib62** substrate (400 nM) was incubated under multiple turnover conditions with *deoxyribose*-**614** (100 nM) at 15 °C (■) and 25 °C (○). The number of substrate turnovers was calculated by multiplying the percent of substrate cleaved by the initial substrate concentration and dividing by [*deoxyribose*-**614**].

ments indicate that the rate of E·S dissociation is greater than the rate of the chemical step ($k_{cat(bi)} \ll k_{-1(bi)}$).

*Dependence on Temperature of Deoxyribose-**614** Cleavage.* The temperature dependence of initial rates for ribose-**614** cleavage under trans cleavage conditions is shown in Figure 8. The rate is lower by a factor of 2.5 at 25 °C than at 15 °C and falls dramatically at higher temperatures. Thus, as true for many biological catalysts, it appears as if the catalyst−substrate complex required for trans cleavage unfolds (or dissociates) at higher temperatures.

The rate of cleavage of *ribose*-**614** under trans cleavage conditions is essentially the same between 4 and 15 °C and 2.5-fold greater than the rate at the selection temperature (25 °C). Similarly, the rate for cis cleavage of *ribose*-**614** is essentially the same at 4 and 25 °C (Supplemental Figure 16 of the Supporting Information). The rate of the chemical step is expected (as an approximation) to increase 2-fold for every 10 °C increase in temperature (*16*). Thus, it appears as though the overall rate of catalysis is largely affected by the folding/association step and not the chemical step.

The rate of cleavage of *ribose*-**lib62** in trans by *deoxyribose*-**614** in single-turnover experiments is comparable at 15 and 25 °C, however (Supplemental Figure 17 of the Supporting Information). Similar experiments performed under multiple-turnover conditions reveal a rate enhancement at lower temperatures during cleavage of the first substrate, followed by cleavage of additional substrates at a slower rate (Figure 9). This "burst phase" seen under multiple turnover conditions at 15 °C is not seen at 25 °C (Supplemental Figure 14 of the Supporting Information). This indicates that lower temperatures increase the initial rate by stabilizing intermolecular association between the enzyme and substrate or, perhaps, through greater stability of the folded form of the enzyme. This stabilization presumably also slows the dissociation of product from enzyme to within the range of $k_{-1(bi)}$ and therefore reduces the rate for multiple turnover after the first turnover.

Predictions of the Energetically Favored Secondary Structure Are Not Supported by Experimental Data. The ability of **614** to cleave in cis is not particularly surprising, because this is the function for which the DNAzyme was selected. It is therefore interesting that **614** is able to cleave various substrates in trans and that the apparent first-order rate constant at saturation for trans cleavage is 4-fold higher than the first-order rate constant for cis cleavage. The ability of **614** to cleave the *cat* + *ribose* primer, as well as a library of molecules containing the *cat* + *ribose* primer, suggests that **614** has a binding motif that pairs with a part of the *cat* + *ribose* primer common to all substrates, thus positioning a separate catalytic motif near the adenine riboside cleavage site.

Chemical modifications specific for single-stranded DNA were used to probe secondary structure. *Deoxyribose*-**614** (300 nM) was folded overnight with and without excess unlabeled *cat* + *deoxyribose* substrate (10 μM). The mixtures were then treated with either potassium permanganate (which modifies thymine) or dimethyl sulfate (which, at high salt concentrations, modifies guanine) for 2 and 5 min. Recovered samples were resolved by PAGE−urea next to a 10-bp ladder.

All thymine and guanine nucleotides reacted to a degree with their respective reagents, indicating that either some **614** is not folded at all or adopts multiple conformations. Nonetheless, T44, T46, T74, G33, G41, G65, G71, and G75 all demonstrated some degree of differential protection (numbers refer to the sequence of **614** shown in Figure 3). The pattern of protected and sensitive positions observed under chemical modifications is not simultaneously compatible with any single structure predicted for **614** folded in cis or trans. This suggested that either a mixture of conformers exists or none of the predicted structures accurately reflect the single true structure of **614**.

Likewise, each of the eight lowest free-energy structure predictions made by Mfold was examined by generating mutations that would disrupt critical helixes. In no case could a loss of function arising from a nucleotide replacement be rescued by a compensatory mutation predicted by Mfold (data not shown). This suggests that either (a) none of the predicted conformations dominated or (b) the mutated nucleotides are involved in tertiary interactions that are not amenable to rescue by compensatory mutations that restore Watson−Crick base pairing.

It is interesting to note that many of the structures reported for in vitro selected DNAzymes are based on unverified predictions using programs such as Mfold. Although such programs have been useful for predicting structures for many RNA and DNA molecules, this does not appear to be the case with **614**.

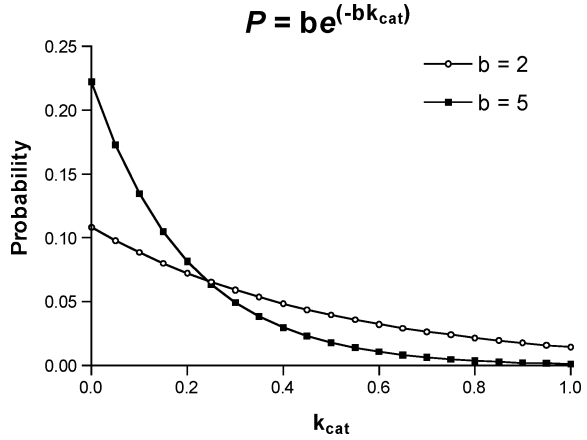

FIGURE 10: Univariate statistical distribution plotting the probability of encountering a catalyst with a particular k_{obs} as a function of k_{obs}, for two catalysts, one with a better pool (○, exponential function with $b = 2$) and the other with a poorer pool (■, exponential function with $b = 5$). In each case, the area under the line sums to unity. Because good catalysts are scarce in the initial library relative to poor catalysts and excellent catalysts are scarce relative to good catalysts, this distribution is a decreasing function of k_{obs}. The distribution shown is exponential; the true nature of the distribution in any particular space is, of course, unknown. Key questions in in vitro selection ask whether this curve is exponential, zipfian, or best captured by mathematical approximations having multiple parameters.

DISCUSSION

In vitro selection experiments offer the possibility of learning how molecular behavior is distributed within a sequence space defined by the building blocks of a biopolymer, in this case DNA. Structures within DNA sequence space are countable. For standard DNA, 4^n sequences exist, where n is the length of the biopolymer. This distribution is relevant to issues as diverse as the origin of life and biomedicine. First, we wish to know how large a hypothetical prebiotic pool of random nucleic acid sequences must have been to contain the physical and catalytic requirements for life. Second, we may want therapeutic or diagnostic DNAzymes and need to know the likelihood of obtaining these from selection experiments. In both, we may ask whether added compounds (including divalent metal ions or other cofactors) increase the likelihood of obtaining catalysts.

The answers to such questions might exploit the language of univariate statistical analysis (Figure 10, see refs *17* and *18*). A distribution function $P(k_{obs})$ relates the probability of finding a molecule with a particular catalytic power, k_{obs}, to k_{obs} itself. Because good catalysts are presumed to be scarce in the initial library relative to poor catalysts and excellent catalysts are presumed to be scarce relative to good ones, this distribution is expected to be a decreasing function of k_{obs}. Using such analyses, a better pool is defined as one having a distribution shifted to the right (Figure 10). Adding a useful cofactor to the pool should shift the distribution to the right as well.

To address such "big" questions, catalysts being examined must be sufficiently well-behaved that their behavior can be quantitatively analyzed. Many DNAzymes are not well-behaved, including (upon first inspection) **614**. In particular, the reaction of **614** did not go to completion. Approximately 35% of the starting material is unreacted even after prolonged incubation. This makes quantitative analysis difficult.

Similar behaviors are well-known in the literature of nucleic acid catalysts. Hammerhead ribozymes, for example, are frequently reported to cleave to only 40−60% at the plateau [reviewed by Stage-Zimmerman and Uhlenbeck (*5*), see also Kore et al. (*6*)]. DNAzymes with ribonuclease activity and deoxyribonuclease activity are also frequently reported with self-cleavage plateaus of 25−65% (*7*−*10*). This behavior must be understood before any quantitative analysis can begin.

This paper accounts for the incomplete cleavage (the plateau) displayed by DNAzyme **614**. Approximately 6−7% of the total *ribose*-**614** sample does not cleave because it is missing the adenine ribonucleoside linkage, which is the site of cleavage. Approximately 9−13% of the total sample appears to fold into an unreactive conformation, which repopulates the active conformation via a cycle of denaturation and renaturation. As much as 15% of the unreacted material at the plateau appears to be sequences containing mutations introduced during amplification or the synthesis of template. These numbers sum to 30−35%, approximately the amount of DNAzyme left uncleaved at the plateau.

Less than 5% of the plateau in our experiments can be attributed to the presence of DNA complementary to the catalyst. Nevertheless, our results show the importance of efficient removal of the complementary strand. Contamination by 10% of the complementary strand has little effect on initial cleavage rate or cleavage plateau, while greater contamination can greatly reduce the cleavage plateau and therefore estimates for cleavage rates. For this reason, we believe both asymmetric PCR and exonuclease degradation are superior to column purification (under strong base) as a way of eliminating the complementary strand.

Given this understanding of the progress curve of the reaction undergone by **614**, we asked whether the features of this DNAzyme reflect the environment under which the DNAzyme was selected. We expected that the presence of Mg^{2+} in the selection would lead to catalytic molecules that used Mg^{2+} as a cofactor. In part, this expectation arose because Breaker and Joyce themselves reported a Mg^{2+}-dependent DNAzyme emerging from their selection. Indeed, the Breaker−Joyce IVS protocol, by using Mg^{2+} as the trigger to begin the selection process, seems to require that the DNAzyme be active *only* with Mg^{2+}.

In addition, this expectation is based on a general view that the catalytic potential of DNA is poor. DNA lacks a range of functional groups, in particular, many of those present in proteins (*19*). In this view, the probability of finding a good catalyst that exploits a useful cofactor (such as Mg^{2+}) is greater than the probability of finding a good catalyst that does not. In terms of the distributions shown in Figure 10, adding Mg^{2+} should shift the distribution to the right.

For both reasons, we were surprised to discover that *ribose*-**614** is as active in the absence of Mg^{2+} as it is in its presence. This behavior was not unique to *ribose*-**614** in this selection. It was also observed for two other deoxyribozymes isolated from the same selection, termed *ribose*-**62** and *ribose*-**616**. A fourth DNAzyme generated in this paper, *ribose*-**625**, was found to be Mg^{2+}-dependent at the temperature used for the selection but evidently not at 4 °C. While this sample is far from statistical, it suggests that the distribution of catalysts in the pool examined does not greatly

favor Mg^{2+}-dependent catalysts over Mg^{2+}-independent catalysts. This, in turn, implies that adding Mg^{2+} to the library does not shift the distribution in Figure 10 greatly to the right.

The emergence from a selection of catalysts that fail to take advantage of available cofactors is not unprecedented. For example, Faulhammer and Famulok report a selection performed in the presence of histidine (20 mM) at a low concentration of Mg^{2+} (0.5 mM) (*8*−*9*). These authors hoped to select a DNAzyme that exploited histidine as a cofactor. They isolated, however, a DNAzyme that was highly active with Ca^{2+} in the absence of histidine. This behavior was selected despite the fact that Ca^{2+} was excluded from the selection. Mg^{2+}, present in the selection, was a poor substitute for Ca^{2+}. At the same time, Roth and Breaker, also seeking a histidine-dependent nucleic acid enzyme, found one (*20*).

Our results differ from those reported by Breaker and Joyce, who analyzed a single, Mg^{2+}-dependent catalyst that emerged from an analogous selection. Breaker and Joyce did not survey their catalysts to determine the ratio of Mg^{2+}-independent and Mg^{2+}-dependent catalysts. Thus, it is conceivable that their study of a Mg^{2+}-dependent catalyst differs from our study of a Mg^{2+}-independent catalyst because of the stochastic nature of the selection experiment.

Other explanations are conceivable, however. Although the concentrations of Mg^{2+} were the same in our selection as the Breaker−Joyce selection, the sequences used by Breaker and Joyce possessed two pairs of self-complementary sequences (each referred to as a "clamp") (*11*). These clamps were introduced by design into the library to anchor the substrate and enzyme regions of the molecule together with a four-base-pair clamp on one side of the cleavage site and a six-base-pair clamp on the other. The combined length of these clamps increased to 15 base pairs following selection.

In the selection experiments reported here, a binding clamp of this length was not introduced by design. This difference, which was not considered to be significant at the outset, may have had consequences. The absence of extensive clamps may transfer selective pressure onto the folding/association step and away from the catalytic step. Thus, selection within a library lacking clamps may not generate as strongly catalysts that exploit cofactors as the selection within a library having clamps. This may explain why the catalysts that we examined are Mg^{2+}-independent, while the catalyst examined by Breaker and Joyce is Mg^{2+}-dependent.

A curious parallel is found when comparing the Faulhammer−Famulok selection experiment cited above (*8*−*9*) and the analogous experiment by Roth and Breaker. The former failed to isolate histidine-dependent DNAzymes; the latter generated several histidine-dependent DNAzymes (*20*). Two differences in their selection protocols appear relevant. The Faulhammer/Famulok protocol included low amounts of $MgCl_2$ (0.5 mM) in addition to the histidine cofactor during selection, while the Roth/Breaker selection did not. Further, the Roth−Breaker libraries included engineered binding clamps, analogous to the clamps in the Breaker−Joyce selection for ribonucleases. The Faulhammer−Famulok libraries did not.

It may be coincidental that selections with clamped libraries in two cases generated catalysts that exploited an external cofactor, while analogous selections with libraries lacking the clamp generated catalysts that did not. These results suggest, however, that the presence of base pairing between the substrate and enzyme portions of the nucleic acid enzyme may be important to the experimental outcome.

Including clamps between the substrate and enzyme motifs in the DNAzyme appears also to give faster catalysts. The catalyst that Breaker and Joyce examined in detail has a rate constant of 0.12 h^{-1} before reselection; reselection improved this to 1.2−4.6 h^{-1} (*11*). Likewise, the catalyst reported by Santoro and Joyce had rate constants of 6 and 600 h^{-1} before and after reselection (*13*−*14*). The metal−cofactor-independent catalyst reported by Sen and Geyer had rate constants of 0.17 and 0.4 h^{-1} before and after reselection (*7*). In contrast, the rate constants for the metal−cofactor-independent catalysts selected here are considerably smaller (0.015−0.05 h^{-1}, both before reselection).

This paper suggests that if one wishes to obtain a fast catalyst, one should engineer clamps into the sequence. Indeed, Santoro and Joyce found that reducing the length of the clamps (for a DNAzyme selected with clamps) to six base pairs or fewer (on both sides of the clamp) reduced k_{cat} 10-fold for an intermolecular reaction and increased K_m 100-fold (*13*−*14*). On the other hand, to understand catalytic potential in a truly random pool, one is advised not to use engineered clamps. The information in an engineered clamp containing a 14-base-pair duplex is substantial, even considering that the exact bases paired is not important. The specification of 14 nucleotides in a 4 letter alphabet is $4^{14} \approx 10^8$. This is significant relative to the size of a typical library (10^{13} molecules).

What do these experiments tell us about sequence landscape and evolvability within DNA libraries, where the reaction sought is the cleavage of a ribonucleotide linkage? Many sequence variants of **614** were isolated that differed at only one or two positions. Most of these exhibited cleavage rates that were more than an order of magnitude slower than that for **614** itself. In contrast, variants of **614** changed at one or two sites were isolated following additional rounds of selection. These generally had rates that were an order of magnitude faster than those for the original **614**. The fact that a 100-fold variation in rates arising from only minor changes in sequence suggests a degree of ruggedness to the landscape relating sequence space to catalysis in this system (*21*).

What do these experiments tell us about the origin of life? The hypothesis that life emerged as a nucleic acid capable of self-replication (*22*) remains disputed (*23*). The recent discovery of a plausibly prebiotic route to ribose is encouraging the re-examination of this hypothesis, however (*24*). In no case, however, does DNA appear to be a candidate for the first living biopolymer.

To the extent that conformation and catalysis in RNA and DNA are analogous, however, we may offer a few observations. First, binding clamps of sufficient length are unlikely to occur frequently in a prebiotic soup. If binding clamps of 14 base pairs are required (the optimal length estimated by Santoro and Joyce, see ref *14*), it would increase the required size of a prebiotic library by a factor of 10^8. Without extensive clamps, it appears (if this paper can be taken as a model) that catalysis is limited by folding. Folding, in the absence of extensive clamps, occurs more favorably at low temperatures. To the extent that the behavior of **614** is representative, cold temperatures would appear to be more

favorable for a nucleic acid origins of life than high temperatures.

Last, trans cleavage in this system is incidental to selection. It is, however, a likely result of the promiscuous nature of nucleic acid binding. Under the conditions in which a nucleic acid catalyst was evolving, selection likely acted upon a small set of nucleic acid catalysts isolated within a compartment. Significant trans interactions would be possible within the compartment. If a trans reaction is generally associated with a nucleic acid catalyst that is capable of a cis reaction, this may be relevant to the origin of life.

ACKNOWLEDGMENT

We thank Dr. Maurice Swanson for generously offering suggestions and the use of equipment and facilities. We also thank Dr. Alfred Lewin and Dr. Carl Urbinati for many helpful discussions.

SUPPORTING INFORMATION AVAILABLE

Effect of complementary strand on *ribose*-**614** cleavage rate; effect of cleavage products on *ribose*-**614** cleavage and *ribose*-library cleavage; cleavage rate of *ribose*-**614** following plateau and subsequent refolding by gel purification or heating; concentration-dependent cleavage of *deoxyribose*-**614**; competition studies of *ribose*-**614** cleavage; *deoxyribose*-**614** cleavage of various substrates at saturation and below saturation; effect of omitting the slow cool protocol on **614** cleavage; comparison of *ribose*-**614** cis cleavage with the residual *ribose*-**614** cleavage following chase; and effect of temperature on *ribose*-**614** cleavage in cis and *ribose*-**lib62** cleavage by *deoxyribose*-**614**. This material is available free of charge via the Internet at http://pubs.acs.org.

REFERENCES

1. Bartel, D. P., and Szostak, J. W. (1993) Isolation of new ribozymes from a large pool of random sequences, *Science 261*, 1411−1418.
2. Breaker, R. R., and Joyce, G. F. (1994) A DNA enzyme that cleaves RNA, *Chem. Biol. 1*, 223−229.
3. Breaker, R. R. (2000) Molecular biology—Making catalytic DNAs, *Science 290*, 2095−2096.
4. Perrin, D. M., Garestier, T., and Helene, C. (2001) Bridging the gap between proteins and nucleic acids: A metal-independent RNAseA mimic with two protein-like functionalities, *J. Am. Chem. Soc. 123*, 1556−1563.
5. Stage-Zimmermann, T. K., and Uhlenbeck, O. C. (1998) Hammerhead ribozyme kinetics, *RNA 4*, 875−899.
6. Kore, A. R., Vaish, N. K., Morris J. A., and Eckstein, F. (2000) In vitro evolution of the hammerhead ribozyme to a purine-specific ribozyme using mutagenic PCR with two nucleotide analogues, *J. Mol. Biol. 301*, 1113−1121.
7. Geyer C. R., and Sen, D. (1997) Evidence for the metal-cofactor independence of an RNA phosphodiester-cleaving DNA enzyme, *Chem. Biol. 4*, 579−593.
8. Faulhammer, D., and Famulok, M. (1997) Characterization and divalent metal-ion dependence of in vitro selected deoxyribozymes which cleave DNA/RNA chimeric oligonucleotides, *J. Mol. Biol. 269*, 188−202.
9. Faulhammer, D., and Famulok, M. (1996) The Ca^{2+} ion as a cofactor for a novel RNA-cleaving deoxyribozyme, *Angew. Chem., Int. Ed. Engl. 35*, 2837−2841.
10. Carmi, N., Shultz, L. A., and Breaker, R. R. (1996) In vitro selection of self-cleaving DNAs, *Chem. Biol. 3*, 1039−1046.
11. Breaker, R. R., and Joyce, G. F. (1995) A DNA enzyme with Mg^{2+}-dependent RNA phosphoesterase activity, *Chem. Biol. 2*, 655−660
12. Maniatis, T., Fritsch, E. F., and Sambrook, J. (1982) *Molecular Cloning: A Laboratory Manual*, Cold Spring Harbor Laboratory Press, Cold Spring Harbor, NY.
13. Santoro, S. W., and Joyce G. F. (1997) A general purpose RNA-cleaving DNA enzyme, *Proc. Natl. Acad. Sci. U.S.A. 94*, 4262−4266.
14. Santoro, S. W., and Joyce G. F. (1998) Mechanism and utility of an RNA-cleaving DNA enzyme, *Biochemistry 37*, 13330−13342.
15. Zuker, M. (2003) Mfold web server for nucleic acid folding and hybridization prediction, *Nucleic Acids Res. 31*, 1−10.
16. Laidler, K. J., and Peterman, B. K. (1979) Temperature effects in enzyme kinetics, *Methods Enzymol. 63*, 234−257.
17. Johnson, N. L., Kotz, S., and Balakrishnan, N. (1994) *Continuous Univariate Distributions*, Vol 1, 2nd ed., Chapter 21, Wiley, New York.
18. Nelson, W. (1982) *Applied Life Data Analysis*, John Wiley and Sons, Inc., New York.
19. Benner, S. A., Allemann, R. K., Ellington, A. D., Ge, L., Glasfeld, A., Leanz, G. F., Krauch, T., MacPherson, L. J., Moroney, S. E., Piccirilli, J. A., and Weinhold, E. G. (1987) Natural selection, protein engineering, and the last riboorganism. Rational model building in biochemistry, *Cold Spring Harbor Symp. Quant. Biol. 52*, 53−63.
20. Roth, A., and Breaker, R. R. (1998) An amino acid as a cofactor for a catalytic polynucleotide. *Proc. Natl. Acad. Sci. U.S.A. 95*, 6027−6031.
21. Yomo, T. (2002) Molecular evolution in static and dynamical landscapes, *J. Biol. Phys. 28*, 471−482.
22. Rich, A. (1962) in *Horizons in Biochemistry* (Kasha, M., and Pullman, B., Eds.) pp 103−126, Academic Press, New York.
23. Shapiro, R. (1988) Prebiotic ribose synthesis. A critical analysis, *Origins Life Evol. Biosphere 18*, 71−85.
24. Ricardo, A., Carrigan, M. A., Olcot, A. N., and Benner, S. A. (2004) Borate minerals stabilize ribose, *Science 303*, 196.

BI049898L